Observation of exponential spectra and Lorentzian pulses in the TJ-K stellarator

G. Hornung, B. Nold, J. E. Maggs, G. J. Morales, M. Ramisch, and U. Stroth

Observation of exponential spectra and Lorentzian pulses in the TJ-K stellarator

G. Hornung,[1] B. Nold,[1] J. E. Maggs,[2] G. J. Morales,[2] M. Ramisch,[1] and U. Stroth[1]

[1]*Institut für Plasmaforschung, Universität Stuttgart, D-70569 Stuttgart, Germany*
[2]*Department of Physics and Astronomy, University of California, Los Angeles, California 90095, USA*

An experimental investigation of the low-frequency density fluctuations in the plasma edge region of the TJ-K stellarator [N. Krause *et al.*, Rev. Sci. Inst. **73**, 3474 (2002)] finds that the ensemble-averaged frequency spectra exhibit a near exponential frequency dependence whose origin can be traced to individual pulses having a Lorentzian temporal shape. Similar features have been previously observed [D. C. Pace *et al.*, Phys. Plasmas **15**, 122304 (2008)] in a linear magnetized device under conditions in which cross-field pressure gradients are present. The reported observation of such features within the turbulent environment of a toroidal confinement device provides support for the conjecture that the underlying processes are a general feature of pressure gradients. Also presented is the magnetic field strength dependence of the pulse widths and the waiting time distribution between pulses. © *2011 American Institute of Physics*. [doi:10.1063/1.3622679]

I. INTRODUCTION

Presently, there is significant interest[1–11] in understanding the properties of plasma fluctuations at the edge of magnetically confined devices because of their important role in particle and energy transport in a fusion environment. Large density structures exhibiting temporal intermittency[12] and propagating through the scrape-off layer (SOL) have been observed in the DIII-D,[13] HL-2A,[14] and TEXTOR[15] tokamaks to result in approximately 50% of the particle transport. Similar results have also been obtained in several other toroidal confinement devices. Such findings suggest that the underlying physical processes should be carefully examined to better assess the performance of ITER and future fusion devices.

Two analysis tools that are extensively used to extract information about the physical processes leading to edge fluctuations and plasma turbulence are the ensemble-averaged frequency spectrum and the probability distribution function (PDF). It is common experimental practice to extract these quantities from time series of ion saturation current collected by a Langmuir probe at a fixed spatial location in the plasma edge. A survey based on such experimental techniques[5] concluded that the amplitude PDF of edge fluctuations in several different devices exhibits a universal shape that deviates from Gaussian statistics. The authors associated the large intermittent events causing the deviation with spatial structures that they named "avaloids." Deviations of the amplitude PDF from Gaussian statistics have also been reported in another survey[16] of other devices, but these authors associate the deviation with intermittent events related to an interplay of self-organized critically (SOC) and flow-velocity shear.

The search for universal features in the frequency spectrum of fluctuations has been greatly influenced by the pioneering work of Kolmogorov,[17] which suggests algebraic dependencies. As a consequence, most experimental studies[15,16,18–23] choose to display the data in log-log scale and piecewise fits are often made to extract power-law indices that are compared to the Kolmogorov turbulence model, or other plasma dynamical models. However, the log-log display format compresses a large dynamic range of the data and thus it can obscure important underlying features of the fluctuations, as has been recently found in experiments performed in a linear device.[24]

The studies in the large plasma device (LAPD) by Pace *et al.*[24] considered two different situations in which cross-field pressure gradients were created in a magnetized plasma column. One was a pure temperature gradient consisting of a hot electron channel surrounded by a cold plasma. The other was a pure density gradient established at the plasma edge by inserting a metallic limiter, an arrangement closer to the TJ-K studies described in this manuscript. The two systems studied in LAPD had significantly different spatial scales and plasma parameters. Using a log-linear display of the ensemble-averaged, low-frequency power spectrum (below the ion cyclotron frequency), $P(\omega)$, it was found that both systems exhibited an exponential frequency dependence, i.e.,

$$P(\omega) \propto e^{-\alpha\omega}, \qquad (1)$$

where ω is the angular frequency and α^{-1} is a scaling frequency. Furthermore, by examining the individual time traces collected by Langmuir probes, it was determined that the reason for the exponential spectrum was the presence of temporal pulses that exhibited a Lorentzian functional dependence, i.e.,

$$L(t) = \frac{A}{1 + \left(\frac{t - t_0}{\tau}\right)^2}, \qquad (2)$$

where t_0 is the time of peak arrival, τ is the pulse width, and A the peak amplitude.

Since the Fourier transform of the Lorentzian pulse in Eq. (2) is

$$\hat{L}(\omega) = A\tau\pi e^{i\omega t_0} e^{-\omega\tau}, \tag{3}$$

the resulting frequency power spectrum due to a single pulse is an exponential function,

$$P(\omega) = A^2\tau^2\pi^2 e^{-2\omega\tau}. \tag{4}$$

Equation (4) shows that the inverse of the scaling frequency associated with a single pulse is $\alpha = 2\tau$, i.e., the slope of the power spectrum in a log-linear plot is directly determined by the pulse width. This relation provides a consistency test for the phenomena being observed because α and τ are quantities that, in principle, can be independently determined. It should be noted, however, that if the pulses occurring in individual time traces have a broad distribution of widths, the ensemble-averaged spectrum will deviate from an exponential curve with a single slope (in linear-log display), even if all the individual pulses strictly exhibit a Lorentzian shape. Thus, observation of nearly exponential behavior in an experiment is a strong indication of two facts: the pulses have a fairly narrow width distribution and their shape is quite close to a Lorentzian.

The possibility that the shape of individual pulses follows other functional forms that display similar quadratic behavior near their peak value (e.g., Gaussian or sech^2 functions) can be discriminated by the shape of the power spectrum. The key difference between Lorentzian-shaped pulses and others is the long tails of the Lorentzian. The tails are responsible for the exponential behavior of the power spectrum. When power spectra modeled on Lorentzian pulses deviate from exponential, due to a broad distribution of pulse widths, they have an upward curvature. The feature that distinguishes between pulse models is the pronounced downward curvature in the log-linear displays of the power spectra corresponding to pulses with shapes other than a Lorentzian, as shown in Fig. 16 of Ref. 24. Because the sign of the curvature of the spectrum associated with, for example, a Gaussian pulse shape is opposite from that resulting from a distribution in the widths of Lorentzian pulses, as shown in Fig. 17 of Ref. 24, it is possible to distinguish between these two pulse shapes when deviations from a perfect exponential are observed.

In summary, the shape of the pulses in edge density fluctuations can be determined by fitting individual pulses to various shapes. A distribution of individual pulse widths can be obtained. This fitting process can be obscured, however, by other fluctuations in the plasma, which distort the fundamental pulse shape, and, on an individual pulse basis, different shapes may give acceptable fits. The feature that ultimately distinguishes between pulse shapes is the power spectrum. Only Lorentzian pulses give the correct power spectrum whose shape agrees with the distribution of pulse widths obtained from individual fitting.

The present observational study tests the conjecture that exponential spectra, and the associated Lorentzian pulses, are a general feature of magnetized plasmas with cross-field pressure gradients by analyzing the properties of the density fluctuations in the edge region of the TJ-K stellarator. The manuscript is organized as follows. Section II outlines the experimental setup. The temporal pulse shape is examined in Sec. III, while the pulse statistics are reported in Sec. IV. Section V analyzes the power spectra. A discussion and conclusions are provided in Sec. VI.

II. EXPERIMENTAL SETUP

The fluctuation measurements were performed in the TJ-K stellarator at Stuttgart University. Details about the operation of the device and its physical characteristics are given in Ref. 25. The major and minor radii of this toroidal device are $R_0 = 0.6$ m and $a = 0.1$ m, respectively. Low-temperature plasmas are generated in TJ-K by the application of 1 kW of microwave power, at 2.45 GHz (for a magnetic field of 72 mT) and 8.25 GHz (for a magnetic field of 244 mT), to a background of neutral helium gas at nominal pressures of $p_n \approx 11.2$ mPa. This method yields steady-state plasmas of up to 40 minutes duration having electron densities $n_e \approx 10^{17}$ m^{-3}, with electron temperatures $T_e \approx 7$ eV and relatively cold ions with temperatures $T_i \leq 1$ eV.

In the present study, two large poloidal plates (i.e., limiters) are used to define the separatrix. They create an extended SOL, with a homogeneous connection length of approximately $L_\parallel = 1$ m and a relatively uniform density profile. The data presented here samples fluctuations in this homogeneous SOL, and also in the nearby edge region of the core plasma that exhibits a larger density gradient. The region labeled "inhomogeneous SOL" is so named because the connection length is inhomogeneous there. Data are not collected in this region. A two-dimensional sketch (R, Z) of the various plasma regions is shown in Fig. 1, in which the location of the Langmuir probe used to collect the ion saturation current is illustrated.
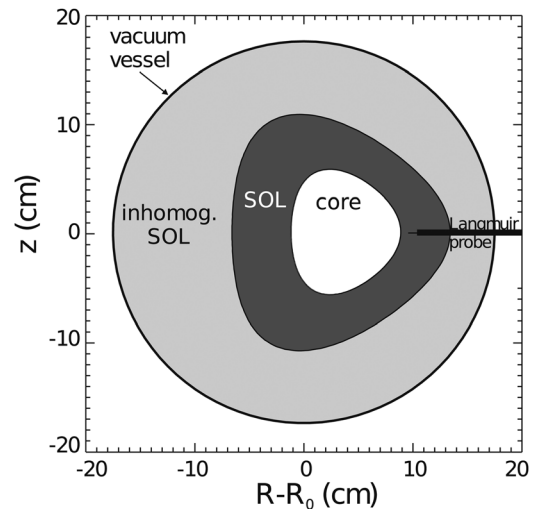

FIG. 1. Two-dimensional schematic (R, Z) of plasma in TJ-K stellarator indicating the core confined plasma (white), the homogeneous scrape-off layer SOL (dark) generated by a poloidal limiter, and surrounding inhomogeneous SOL (light gray). A Langmuir probe inserted from the right samples fluctuations in the homogeneous SOL and the gradient region of the core plasma adjacent to the separatrix.

The Langmuir probe used to collect ion saturation current, I_{sat}, consists of a 300 μm tungsten wire, isolated by a ceramic tube of 2 mm outer diameter, and having a free tip 2 mm in length. Measurements were taken with a radial spacing of $\Delta r = 5$ mm, during intervals of 0.5 s with a 1 MHz sampling frequency yielding 512 000 data points at each radial position.

Figure 2(a) displays the radial dependence of the time-averaged value of the ion saturation current, $\bar{I}_{sat}$, for two strengths of the confinement magnetic field, B. Low-field corresponds to 72 mT and high-field to 244 mT. The zero value along the horizontal axis identifies the location of the separatrix generated by the poloidal limiters. It is seen that the higher magnetic field results in a larger peak density and steeper radial density profile within the core plasma, i.e., in the region $r - r_{sep} < 0$. But the density in the homogeneous SOL, i.e., the region $r - r_{sep} > 0$, is not altered by the larger field value. The increase in density of the core plasma is attributed to a reduction in the turbulent transport associated with a reduced size of the turbulent eddies, which was shown in a previous study[26,27] to scale inversely with the magnetic field strength, i.e., as $\sim 1/B$.

Fig. 2(b) displays the amplitude probability distribution functions (PDFs) of fluctuations in ion saturation current, $\tilde{I}_{sat}$, for the two magnetic field strengths studied. The black curve corresponds to the high magnetic field case and the red curve to the low-field case. The green curve is the result predicted for a Gaussian distribution and is provided as a reference to illustrate the deviations in the observed PDFs. The radial position where the PDFs were measured is indicated by the arrow in Fig. 2 and corresponds to $r - r_{sep} = 0.5$ cm within the homogeneous SOL. Since in TJ-K it has been determined that temperature fluctuations are small, the fluc-

tuations contributing to $\tilde{I}_{sat}$ are predominantly density fluctuations.

It is seen from Fig. 2(b) that the amplitude PDFs for both magnetic field strengths deviate from Gaussian statistics. The observed PDFs are asymmetric and indicate a preponderance of events having excess density above the mean value. These enhancements in density are manifestations of positive pulses that transport plasma density outward from the edge of the core plasma into the SOL region. The following sections report the temporal shape, the power spectra, and the waiting time of the positive pulses observed.

III. TEMPORAL PULSE SHAPE

Since the time series of the ion saturation current contains a mixture of various plasma processes (e.g., coherent drift-wave fluctuations, flows), a search algorithm must be implemented in testing for the presence of individual Lorentzian pulses. The technique used here is based on an amplitude threshold that identifies pulses having an amplitude range larger than a selected threshold. That is, for a pulse to be selected, the difference between the pulse maximum and its first minimum must exceed the threshold value. This method automatically rejects many possible Lorentzian events having smaller amplitude than the threshold value, and, the method is not a filter; Lorentzian pulses appear embedded within other phenomena and are naturally distorted. The threshold amplitude range chosen for the analysis is 1.5 σ_{Isat}, where σ_{Isat} represents the standard deviation in fluctuating ion saturation current $\tilde{I}_{sat}$ for each case considered. Several threshold values were tested and it was found this choice is the smallest value for which the statistical properties of the pulses remain unchanged.

A complementary technique to the threshold detection method is the auto-conditional average (ACA).[28] In this procedure an individual pulse is first identified by the threshold method and a segment of data, centered around the pulse peak, is recorded. The temporal length of each recorded segment is 100 μs, which is much longer than the typical pulse width. By averaging over a large number of such pulse subsets, it is possible to construct an average pulse shape. This method emphasizes the coherent features of the process by removing most of the random background fluctuations.

To test the Lorentzian character of the individual pulses, each pulse that exceeds the threshold amplitude is fitted with a function of the type shown in Eq. (2), but with the values of A, t_0, and τ determined by a least square fit. The length of the typical time record sampled is 0.5 s., which yields hundreds of candidate pulses for the low magnetic field case and several thousand for the high-field case. The reason for the larger number of candidate pulses extracted, is that, for the high-field case, the amplitude of the pulses is systematically larger, as seen from the amplitude PDFs in Fig. 2(b).

Figure 3 displays typical examples of a large survey of individual pulses extracted by the threshold method. For each pulse, the least-square fit was performed on the time interval between local minima before and after the pulse maximum. The dark dots represent experimental measurements and the solid red curves are the corresponding fits by
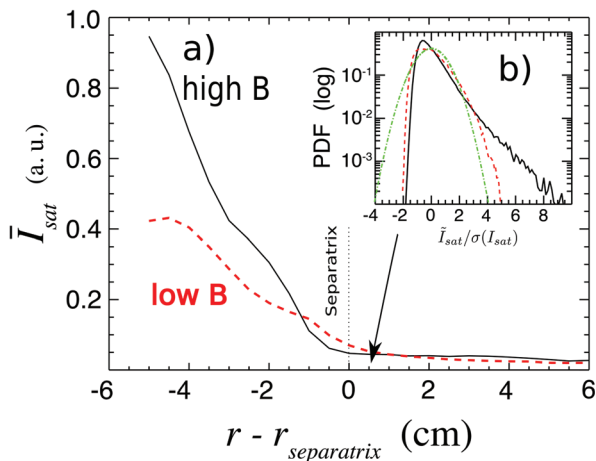

FIG. 2. (Color) (a) Radial dependence of ion saturation current (in arbitrary units) along the midplane direction indicated by the Langmuir probe in Fig. 1. Radial distance is expressed relative to the separatrix. Solid black curve is obtained for the high magnetic field case of 244 mT and the dashed red curve for the low-field case of 72 mT. Insert (b) amplitude probability distribution functions of fluctuations in ion saturation current (log-linear scale). Black curve is the measured PDF at the radial position indicated by the arrow for high magnetic field and the red curve is for low-field. PDFs show an extended tail corresponding to positive pulses. Green curve is a comparison Gaussian function that illustrates the non-Gaussian deviations. Amplitude fluctuations are scaled to the root-mean square values (sigma).
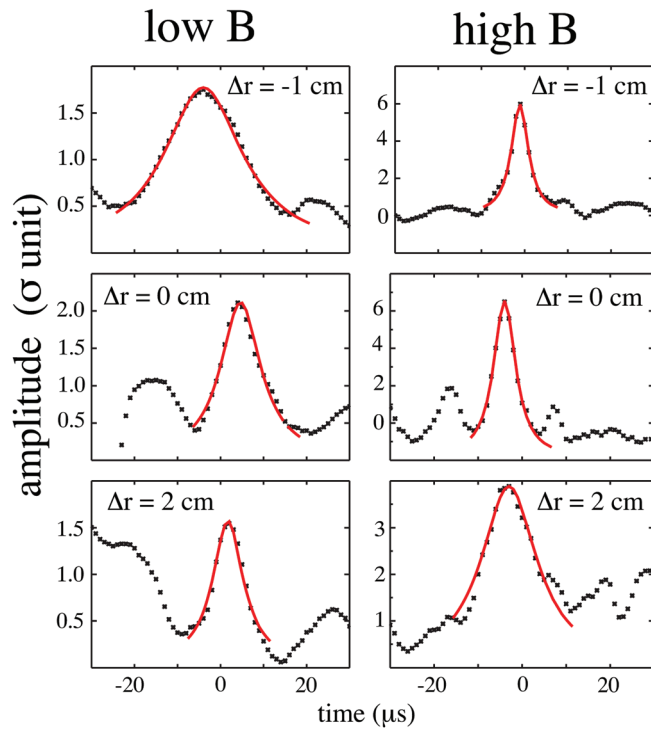
FIG. 3. (Color) Examples of positive pulses whose amplitude exceeds a threshold value $\tilde{I}_{sat} > 1.5\,\sigma_{Isat}$. Left panels are for low-field (72 mT) and right for high-field (244 mT), i.e., variation by a factor of 3.4. Top panels are in the core plasma gradient region, center panels are close to the separatrix, and bottom are in the SOL. Dark dots are measurements and red curves are Lorentzian functional fits.
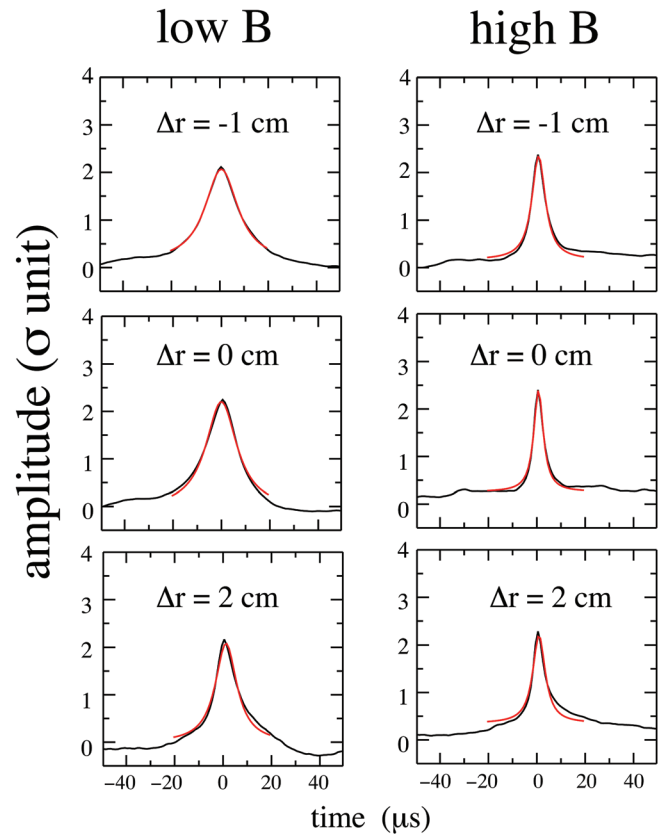

FIG. 4. (Color) Comparison of Lorentzian functional fits (red curves) to the pulse shapes obtained by the auto-conditional averaging method. The fit is only shown over the time interval from -20 μs to $+20$ μs. Panels are arranged as in Fig. 3.

Lorentzian functions. Data obtained for the two magnetic field strengths at three representative radial positions are shown: $\Delta r = -1$ cm corresponds to the region to the left of the separatrix in Fig. 1, i.e., in the edge gradient of the core plasma; $\Delta r = 0$ cm is slightly to the right of the separatrix; $\Delta r = 2$ cm is well inside the homogeneous SOL. It is seen from Fig. 3 that the Lorentzian functional fits provide a good description for the shape of the pulses that exceed the threshold value ($\tilde{I}_{sat} > 1.5\sigma_{Isat}$). It is also demonstrated that this agreement holds over a factor of 3.4 in the strength of the confinement magnetic field that includes plasmas of different peak density and edge gradients. Furthermore, it is found that the pulse shape is not a unique property of a spatial location. The Lorentzian pulses are observed at the edge of the core plasma as well as in the homogeneous SOL layer. Another noteworthy property of the pulses is that the Lorentzian character does not change over a factor of 4 in their relative peak amplitude (scaled to σ_{Isat}), as seen by comparing the right and left panels in Fig. 3.

A test of the Lorentzian fit to the shapes generated by the ACA technique is shown in Fig. 4, where the black curves represent the information extracted from the measurements and the red curves are Lorentzian fits. In applying this method an off-set is added as an additional fit parameter. Here, the fits were performed on a constant time interval ±20 μs around the pulse maximum, and thus, for wide pulses, the long Lorentzian tails are not displayed. The radial positions and magnetic field strengths are the same as in Fig. 3, and the pulse selection uses the same threshold values.

Again, it is seen that the Lorentzian functional fits provide a good representation of the average pulse shape extracted from the ACA method over a broad set of conditions. What the ACA does is remove some of the oscillatory features that distort the Lorentzian pulse when sampled on an individual basis, as seen by comparing Figs. 3 and 4. The ACA signal is rather flat before and after the peak of the pulse, thus suggesting that the pulses correspond to individual structures without significant precursors or trailers. From Fig. 4 it can be seen that, at each radial position, the width of the average Lorentzian pulse decreases with increasing magnetic field. This observation is quantified in the discussion of the PDFs in Sec. IV. An expected consequence of the shorter pulse width is that the ensemble-averaged frequency spectrum should exhibit more power at higher frequencies. Thus it is possible to identify an exponential decrease, over a larger frequency range, for the higher magnetic field case than for the low-field case. Such a feature is shown in Sec. V.

IV. PULSE STATISTICS

There are two quantities related to the Lorentzian pulses that warrant a statistical study, namely the pulse width τ and the waiting time between two successive pulses, Δt.

Figure 5 displays the PDF of the pulse widths for the same range of radial positions and magnetic fields corresponding to the sample pulses shown in Fig. 3. The average pulse width associated with each PDF is given within each
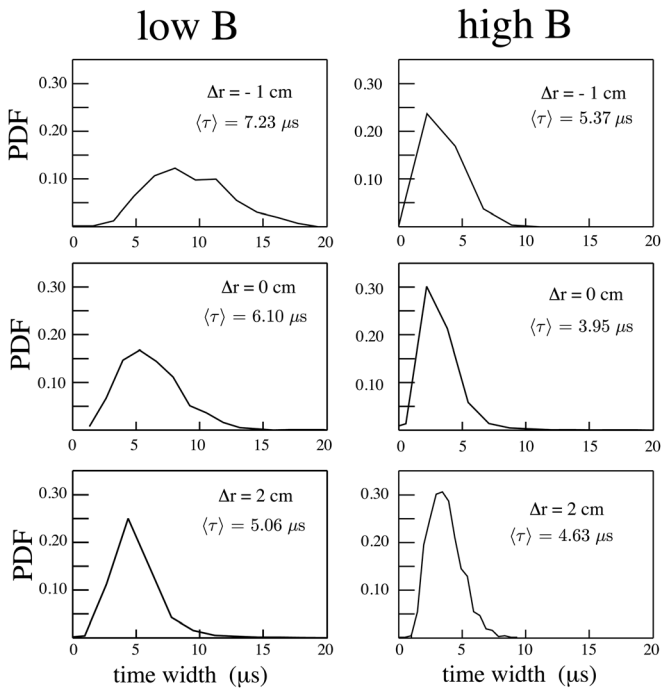
FIG. 5. Probability distribution functions of pulse width τ defined by Eq. (2). Pulses exceed the threshold condition $\tilde{I}_{sat} > 1.5\sigma_{Isat}$ and individual examples are given in Fig. 3. Panels are also arranged as in Fig. 3. The average pulse width for each radial position and magnetic field are given in the corresponding panel. The average width is seen to decrease with increasing magnetic field for all radial positions.
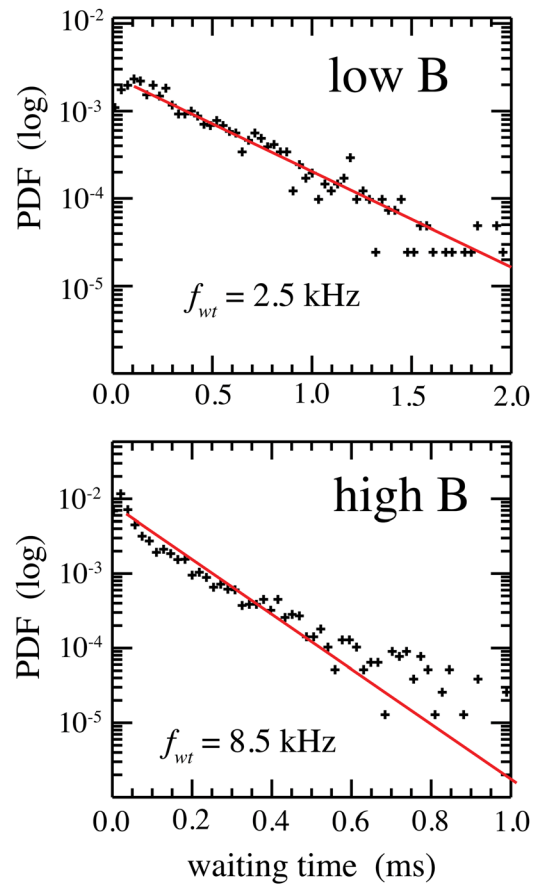

FIG. 6. (Color online) Probability distribution functions for the waiting time between successive pulses that exceed the threshold value $\tilde{I}_{sat} > 1.5\,\sigma_{Isat}$ at the radial position indicated by the arrow in Fig. 2. Top panel is for low magnetic field and bottom for high-field. Both cases exhibit an exponential decay whose characteristic frequency f_{wt} is given in each panel.

panel. It is seen from Fig. 5 that the distribution of pulse widths for low magnetic field is systematically broader than that for the high-magnetic field case, for all radial positions. Also, it appears that the average pulse width has a very weak dependence on radial position. A consequence of these parameter dependencies is that the fit to the ensemble-averaged spectrum by a straight line with a single slope (in a log-linear plot) should work better for the higher magnetic field case, as is shown in Sec. V.

It should be noted that the effective frequencies associated with the average pulse widths shown in Fig. 5 range from the lowest value of 138 kHz at low-field, to the highest value of 253 kHz at high-field. Both of these are substantially larger than the typical frequencies of unstable drift-waves, but still small compared to the ion cyclotron frequency. Thus the temporal widths of the Lorentzian pulses observed are a fraction of a cycle of a characteristic drift-wave, but are still within the domain of $E \times B$ dynamics.

The PDF of the waiting time provides information about the generation mechanism of the pulses. The waiting time Δt is defined as the time between the maxima of two successive pulses selected by the threshold criteria. It is intuitive to expect that generation by a long-lived, coherent drift-wave mode would lead to a narrow distribution with values related to the mode frequency, while a turbulent random process should be reflected in a broad distribution. Figure 6 displays the related PDFs for density fluctuations measured at the position in the SOL indicated by the arrow in Fig. 2, i.e., 0.5 cm away from the separatrix. The threshold amplitude used to extract the pulses for the low and high-field cases is again

$1.5\,\sigma_{Isat}$. The largest values of the waiting time PDF (i.e., the largest number of pulses) are achieved around 60 μs for low-field and 15 μs for high-field, corresponding to about 10 and 4 pulse widths, and yielding an effective inter-pulse frequency of 17 kHz and 67 kHz. This range of frequencies is compatible with that of unstable drift-waves, and is, apparently, the time scale displayed by the largest number of pulses.

It is seen from Fig. 6, for high and low-field, that for large Δt the PDF exhibits an exponential dependence,

$$PDF(\Delta t) \approx f_{wt}e^{-f_{wt}\Delta t}, \qquad (5)$$

with $f_{wt} \approx 1/\langle \Delta t \rangle$; a relation which holds for threshold values from $1.5\sigma_{Isat}$ to $5\sigma_{Isat}$. The observed values are $f_{wt} = 2.25$ kHz for low-field and $f_{wt} = 4.38$ kHz for high-field, which are smaller than typical drift-wave frequencies. However, the ratios of the frequency of largest probability to the average frequency of events are 6.8 and 7.9 for low and high-field, respectively. These ratios are rather close, given that the magnetic field varies by a factor of 3.4. The characteristic frequency values displayed by the inter-pulse statistics are consistent with drift-wave interactions occurring over a similar number of cycles, and may reflect the time interval required for the onset of stochastic behavior.

It should be emphasized that an exponential decay of the PDF of waiting times has been reported in several devices[5,15] and is often interpreted as an indication of systems in a state of self-organized criticality.[29] However, in the present experiment that may not be the case because previous studies in TJ-K (Ref. [30]) have shown that these plasmas are not an SOC system. Specifically, these earlier studies have shown that large-scale pulses in the SOL are generated at the separatrix and originate from drift-wave turbulence inside the confinement region.[31–33] Thus, it is likely that the exponential decay of the waiting time distribution for the pulses sampled in the present study reflects the stochastic nature of drift-wave dynamics in the core plasma.

V. POWER SPECTRA

The ensemble-averaged frequency spectrum of the fluctuations provides a complementary and more sensitive probe for the extended shape of the pulses than individual fits. Since any signal exhibiting a local peak can be fitted over a limited segment by a quadratic function, it is possible for a wide class of functions to provide a somewhat satisfactory fit to the shapes, if the signals are truncated around the peak. However, the frequency spectrum samples the shape of the pulses away from their peak, where the differences in various pulse shapes are most pronounced. Thus, the frequency spectrum distinguishes between pulses having Gaussian or Lorentzian shapes when plotted on a log-linear scale, as mentioned in the introduction. In addition, the frequency spectrum samples pulses having a wide range of amplitudes and widths, not just those that satisfy a threshold condition. The disadvantage, of course, is that the spectrum also contains features unrelated to the pulses of interest.

Figure 7 displays the ensemble-averaged frequency spectra for the same radial positions and magnetic field strengths used in Figs. 3 and 4. Each panel in Fig. 7 displays three different curves, all plotted in log-linear format. The black curve is the experimentally measured spectrum. It contains information about all the physical phenomena that contributes to $\tilde{I}_{sat}$, including the pulses of interest. It is evident that the measured spectra exhibit a nearly linear decay, which implies an exponential frequency dependence. The high magnetic field cases exhibit a better single-slope behavior because, as shown in Fig. 5, the pulse distribution is relatively narrow. The spectra for low-field exhibit a more pronounced deviation from a single-slope, as expected, because the pulses have a broader distribution of pulse-widths. It is of significance that the deviation from a single-slope follows an upward curvature. This upward bend arises because the wider pulses contribute a steeper slope at low frequency while the narrow pulses yield a flatter slope at the higher frequencies, as follows from Eq. (3). The upward bend is an intrinsic feature of Lorentzian pulses that have a broad distribution of pulse widths. However, for the case with the narrowest pulse width distribution the direct fit of a single slope to the spectrum (in a log-linear plot) yields a pulse width $\tau = 4.39 \ \mu$s while the average pulse width obtained by the ACA is $\langle\tau\rangle = 3.95 \ \mu$s, which means the power spectrum slope is consistent with the observed average pulse width.
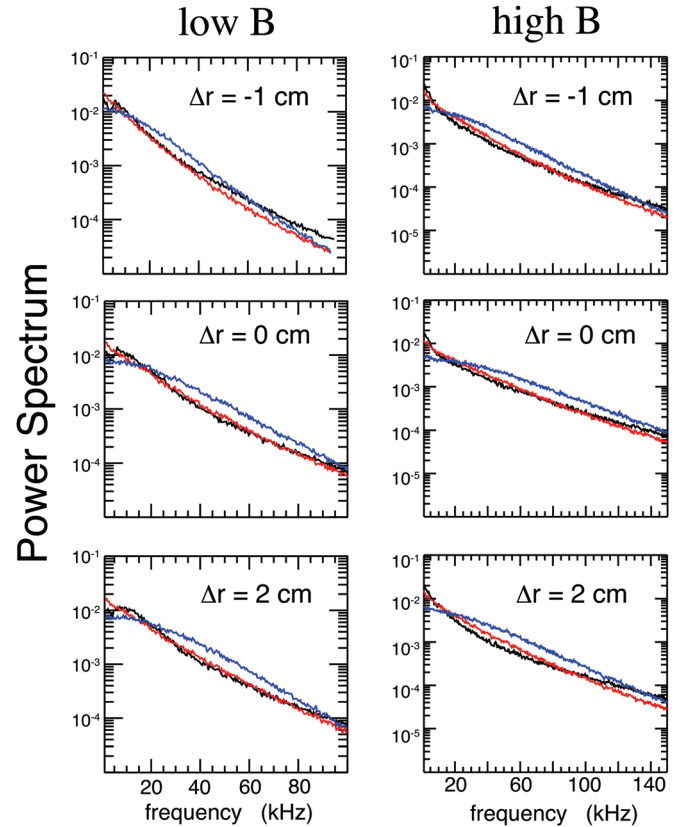

FIG. 7. (Color) Frequency spectrum of fluctuations in ion saturation current from time records of 0.5 s duration. Display is in log-linear scale. The panels are arranged as in Fig. 3. The black curve is the measured spectrum. The red and blue curves are numerically constructed spectra from a synthetic time series in which pulses exceeding the threshold condition are fitted by mathematical functions. The red curves correspond to Lorentzian fits and the blue to Gaussian fits. It is seen that the Lorentzian fits closely reproduce the measurements. In addition, as the distribution of Lorentzian pulse widths becomes narrower, as per Fig. 5, the spectra more closely display exponential frequency dependence with a single scaling frequency.

To test, in more detail, the connection between the exponential spectra and the shape of individual pulses, a comparison-spectrum technique is implemented. The concept consists of first identifying from the time series those pulses that exceed a threshold amplitude range of $1.5 \ \sigma_{Isat}$, as is done in generating Figs. 3 and 4. The extracted pulses are then fit by the functional shape to be tested. Here, we test the Lorentzian of Eq. (2) and a possible Gaussian candidate. The parameters of each Lorentzian and of each Gaussian are determined by a least square fit. From these fitted pulses the ones with the lowest standard deviation (smallest χ^2) are selected. This corresponds to about 30% of the total pulses initially identified, but it turns out this reduced sample set is sufficient to reproduce the experimentally observed spectra. For comparison to data, a synthetic time series 0.5 s long is reconstructed using the extracted fitting parameters (width, amplitude, occurrence time) of the pulses that satisfy the criteria given above. An ensemble averaged power spectrum is then calculated from 250 subsets (each 2 ms long) of the synthetic time interval, each containing 2048 points. The size of the subset was chosen to ensure that each subset contains at least 1 pulse. The average number of pulses per subset is about 3 in the low-field case and 10 for the high-field case.

This process results, for the Lorentzian fit, in the red curve and, for the Gaussian fit, in the blue curve. Both curves are included in the displays of Fig. 7 and are to be judged by how well they reproduce the measurements represented by the black curve.

It is seen in all the panels of Fig. 7 that the red curve closely follows the experimentally observed spectrum. The prediction based on Gaussian pulses, the blue curve, fails to properly describe the spectral measurements. Very significantly, the Gaussian pulses result in a systematic downward curvature that is the opposite to the curvature exhibited by the data (i.e., upward) for the cases in which a broad distribution of pulse widths is present.

VI. DISCUSSION AND CONCLUSIONS

This observational study has examined the ensemble-averaged spectra of density fluctuations present at the edge of a toroidal confinement device, the TJ-K stellarator. It is found that the spectra exhibit a near exponential frequency dependence, for frequencies below the ion cyclotron frequency, over a factor of 3.4 variation in the strength of the confinement magnetic field. The near exponential frequency dependence has been found to arise from individual pulses whose temporal shape, as recorded by a Langmuir probe, follows a Lorentzian functional dependence. The link between the Lorentzian shape and the exponential behavior has been conclusively established by the construction of synthetic time series in which measured large pulses have been replaced by Lorentzian functions. This procedure closely reproduces the measured spectra while attempts to represent the pulses with Gaussian functions show significant deviations. Individual pulses, as well as pulses generated by the ACA technique, can be fit well by Lorentzian functions. For the cases in which the distribution of pulse widths is relatively narrow, the average temporal width of the Lorentzian pulses is found to be consistent with the independent values obtained by fitting the spectra with a straight line in a log-linear plot.

The deviation of the measured spectra from an exponential dependence with a single scaling frequency has been traced to the fact that the Lorentzian pulses display a distribution of pulse widths. It is found that the width distribution becomes narrower with increasing field strength and, accordingly, the measured spectra can be better approximated by an exponential with a single scaling frequency. This implies that in devices with relatively larger magnetic fields the fluctuations should display pure exponential spectra.

It has been found that the average temporal width of a Lorentzian pulse is a fraction of the period of a characteristic drift-wave, while the peak of the waiting time PDF occurs at a time about equal to the drift-wave period. However, the distributions of inter-pulse times exhibit an exponential decay with characteristic times that are much longer than a drift-wave period. These three time scales are clearly separated. They represent, respectively, the flow structures produced by drift wave dynamics, the drift waves themselves and the transport processes modulating the drift wave amplitudes.

By comparing the present observations to the results found in the LAPD linear device, one finds significant similarities. For the limiter-edge configuration, which is closer the present study, it is found in LAPD (Ref. 10) that the average pulse width decreases with increasing magnetic field, and also the distribution of pulse widths becomes narrower. Both these dependencies are clearly observed in TJ-K. But in absolute terms, the width distribution of the pulses in TJ-K are broader and thus result in exponential spectra that are not as well fit with a single scaling frequency, as in LAPD. Another significant similarity is that the pulses are observed over an extended radial domain that includes both the gradient region of the core plasma and the SOL, as seen in Fig. 3.

Exponential spectra have been previously observed in other toroidal devices, notably using different diagnostic techniques. Millimeter-wave backscattering from density fluctuations at the extreme plasma edge in the DIII-D tokamak by Rhodes et al.[34] shows exponential spectra with a single slope (in log-linear plot) in their Fig. 5(c) under Ohmic and electron cyclotron heating (ECH) conditions. Although no connection to Lorentzian pulses was established in their study, previous probe studies in the same device by Boedo et al.[6] have reported signals (e.g., Fig. 7(a) of Ref. 6) that can be closely fit by a Lorentzian function. The study of Sattin et al.[35] has reported the observation of exponential spectra obtained with gas puffing imaging diagnostics (GPDI) in the RFX-mod reversed field pinch (Fig. 1(a) of Ref. 35) and also in the Alcator C-Mod tokamak (Fig. 7 of Ref. 35). It is worth noting that in C-Mod the multichord GPDI system was able to measure exponential spectra that extended from the interior confined plasma, across the separatrix, and into the SOL, as is the case in TJ-K.

The study by Pedrosa et al.[22] attempted to identify an universal frequency dependence for edge fluctuations in toroidal devices. The empirical search included devices of different toroidal field strength and sought to identify dependencies having a functional form given by their Eq. (2), i.e., $P(\omega) = P_O g(\lambda \omega)$, where λ is a constant that is device dependent. It is to be noted that the present results indeed belong to this frequency categorization, with the function g corresponding to the exponential function and the constant λ being related to the average width of Lorentzian pulses which are a fraction of the drift-wave period. In searching for the desired function $g(\lambda \omega)$, Pedrosa et al.[22] displayed the data in the popular log-log format motivated by the Kolmogorov studies,[17] as mentioned earlier in Sec. I. Because this display format compresses the frequency scale, it is not possible to directly compare the present results to their Figs. 1(b), 2, and 3(a) since the exponential dependence shows most clearly in a log-linear plot. But it is possible that the exponential function found in the TJ-K device may provide a reasonable fit to those figures, if the data presented by Pedrosa et al.[22] is displayed in log-linear format, and the frequency is scaled to the cyclotron frequency. A publication by Krause et al.,[25] which provided an introduction to the properties and operational characteristics of the TJ-K device, also reported in their Fig. 8(a) a power spectrum of ion saturation current using a log-log format for the purpose of extracting a power law dependency,

as done by many researchers including Pedrosa *et al.*[22] It is now found, in the present study, that the dependence in the low-frequency range corresponds closely to an exponential function and is associated with pulses having a Lorentzian temporal shape.

In summary, the present study in a stellarator device provides further support for the conjecture that Lorentzian pulses and the concomitant exponential frequency spectrum is a general feature of plasmas with cross-field pressure gradients. Because, in TJ-K, it has been previously established that drift-wave turbulence is a dominant factor, it can be further concluded that drift-waves play a key role in the generation of the pulses. Such a concept has been shown to explain[36] the Lorentzian pulses observed in the temperature gradient experiments in LAPD. However, it should be emphasized that, at the present time, there is no analytic calculation or modeling that directly explains why the temporal shape for density fluctuations observed in TJ-K should be Lorentzian. The experimental results reported in this manuscript extend previous observations reported by Pace *et al.*[24] and strongly suggest that this is a topic that merits a detailed theoretical investigation.

[1]H. Tsuchiya, T. Morisaki, V. P. Budaev, A. Komori, H. Yamada, and LHD Experimental Group, Plasma and Fusion Res. **5**, S2078 (2010).

[2]G. Y. Antar, Contrib. Plasma Phys. **44**, 217 (2004).

[3]I. Furno, B. Labit, M. Podestà, A. Fasoli, S. H. Müller, F. M. Poli, P. Ricci, C. Theiler, S. Brunner, A. Diallo, and J. Graves, Phys. Rev. Lett. **100**, 055004 (2008).

[4]D. A. D'Ippolito, J. R. Myra, and S. I. Krasheninnikov, Phys. Plasmas **9**, 222 (2002).

[5]G. Y. Antar, G. Counsell, Y. Yu, B. Labombard, and P. Devynck, Phys. Plasmas **10**, 419 (2003).

[6]J. A. Boedo, D. Rudakov, R. Moyer, S. Krasheninnikov, D. Whyte, G. McKee, G. Tynan, M. Schaffer, P. Stangeby, P. West, S. Allen, T. Evans, R. Fonck, E. Hollmann, A. Leonard, A. Mahdavi, G. Porter, M. Tillack, and G. Antar, Phys. Plasmas **8**, 4826 (2001).

[7]A. Fredriksen, C. Riccardi, L. Cartegni, and H. Pecseli, Plasma Phys. Controlled Fusion **45**, 721 (2003).

[8]B. A. Carreras, R. Balbin, B. van Milligen, M. A. Pedrosa, I. García-Cortes, E. Sánchez, C. Hidalgo, J. Bleuel, M. Endler, H. Thomsen, A. Chankin, S. Davies, K. Erents, and G. F. Matthews, Phys. Plasmas **6**, 4615 (1999).

[9]C. Hidalgo, B. P. van Milligen, and M. A. Pedrosa, C. R. Phys. **7**, 679 (2006).

[10]T. A. Carter, Phys. Plasmas **13**, 010701 (2006).

[11]O. Grulke, J. L. Terry, B. LaBombard, and S. J. Zweben, Phys. Plasmas **13**, 012306 (2006).

[12]S. J. Zweben, Phys. Fluids **28**, 974 (1985).

[13]J. A. Boedo, D. L. Rudakov, R. A. Moyer, G. R. McKee, R. J. Colchin, M. J. Schaffer, P. G. Stangeby, W. P. West, S. L. Allen, T. E. Evans, R. J. Fonck, E. M. Hollman, S. Krasheninnikov, A. W. Leonard, W. Nevins, M. A. Mahdavi, G. Porter, G. R. Tynan, D. G. Whyte, and X. Xu, Phys. Plasmas **10**, 1670 (2003).

[14]J. Cheng, L. W. Yan, W. Y. Hong, K. J. Zhao, T. Lan, J. Qian, A. D. Liu, H. L. Zhao, Y. Liu, Q. W. Yang, J. Q. Dong, X. R. Duan, and Y. Liu, Plasma Phys. Controlled Fusion **52**, 055003 (2010).

[15]Y. H. Xu, S. Jachmich, R. R. Weynants, and the TEXTOR team, Plasma Phys. Controlled Fusion **47**, 1841 (2005).

[16]E. Sánchez, C. Hidalgo, D. López-Bruna, I. García-Cortes, R. Balbin, M. A. Pedrosa, B. van Milligen, C. Riccardi, G. Chiodini, J. Bleuel, M. Endler, B. A. Carreras, and D. E. Newman, Phys. Plasmas **7**, 1408 (2000).

[17]A. Kolmogorov, Dokl. Akad. Nauk SSSR **32**, 16 (1941) [reprinted in Proc. R. Soc. London **434**, 15 (1991)].

[18]K. Kamataki, Y. Nagashima, S. Shinohara, Y. Kawai, M. Yagi, K. Itoh, and S.-I. Itoh, J. Phys. Soc. Jpn. **76**, 054501 (2007).

[19]B. Labit, A. Diallo, A. Fasoli, I. Furno, D. Iraji, S. H. Müller, G. Plyushchev, M. Podestà, F. M. Poli, P. Ricci, C. Theiler, and J. Horacek, Plasma Phys. Controlled Fusion **49**, B281 (2007).

[20]M. Škorić and M. Rajković, Contrib. Plasma Phys. **48**, 37 (2008).

[21]V. P. Budaev, S. Masuzaki, T. Morisaki, N. Ohno, N. Asakura, S. Takamura, H. Yamada, and A. Komori, J. Plasma Fusion Res. **3**, S1019 (2008).

[22]M. A. Pedrosa, C. Hidalgo, B. A. Carreras, R. Balbín, I. García-Cortés, D. Newman, B. van Milligen, E. Sánchez, J. Bleuel, M. Endler, S. Davies, and G. F. Matthews, Phys. Rev. Lett. **82**, 3621 (1999).

[23]M. Ramisch, N. Mahdizadeh, U. Stroth, F. Greiner, C. Lechte, and K. Rahbarnia, Phys. Plasmas **12**, 032504 (2005).

[24]D. C. Pace, M. Shi, J. E. Maggs, G. J. Morales, and T. A. Carter, Phys. Plasmas **15**, 122304 (2008).

[25]N. Krause, C. Lechte, U. Stroth, S. Niedner, E. Ascasibar, and J. Alonso, Rev. Sci. Inst. **73**, 3474 (2002).

[26]M. Ramisch, N. Mahdizadeh, U. Stroth, F. Greiner, C. Lechte, and K. Rahbarnia, Phys. Plasmas **12**, 032504 (2005).

[27]M. Ramisch, E. Häberle, N. Mahdizadeh, and U. Stroth, Plasma Sources Sci. Technol. **17**, 024007 (2008).

[28]E. J. Powers, Nucl. Fusion **14**, 749 (1974).

[29]P. Bak, C. Tand, and K. Wisenfeld, Phys. Rev. Lett. **59**, 381 (1987).

[30]N. Mahdizadeh, U. Stroth, C. Lechte, M. Ramisch, and B. Scott, Phys. Plasmas **1**, 3932 (2004).

[31]N. Mahdizadeh, F. Greiner, T. Happel, A. Kendl, M. Ramisch, B. D. Scott, and U. Stroth, Plasma Phys. Controlled Fusion **49**, 1005 (2007).

[32]K. Rahbarnia, E. Holzauer, N. D. Mahdizadeh, M. Ramisch, and U. Stroth, Plasma Phys. Controlled Fusion **50**, 085008 (2008).

[33]T. Happel, F. Greiner, N. Mahdizadeh, B. Nold, M. Ramisch, and U. Stroth, Phys. Rev. Lett. **102**, 255001 (2009).

[34]T. L. Rhodes, W. A. Peebles, J. C. DeBoo, R. Prater, J. E. Kinsey, G. M. Staebler, J. Candy, M. E. Austin, R. V. Bravenec, K. H Burrell, J. S. deGrassie, E. J. Doyle, P. Gohil, C. M. Greenfield, R. J. Groebner, J. Lohr, M. A. Makowski, X. V. Nguyen, C. C. Petty, W. M. Solomon, H. E. St. John, M. A. Van Zeeland, G. Wang, and L Zeng, Plasma Phys. Controlled Fusion **49**, B183 (2007).

[35]F. Sattin, M. Agostini, R. Cavazzana, P. Scarin, and J. L. Terry, Plasma Phys. Controlled Fusion **51**, 095004 (2009).

[36]M. Shi, D. C. Pace, G. J. Morales, J. E. Maggs, and T. A. Carter, Phys. Plasmas **16**, 062306 (2009).